

Spin polarization of electrons in two-photon resonant three-photon ionization

S. N. Dixit,* P. Lambropoulos,* and P. Zoller

Institute for Theoretical Physics, University of Innsbruck, Innsbruck, Austria

(Received 8 August 1980)

We present a theory of spin polarization of electrons ejected from atoms by two-photon resonant three-photon ionization. Our treatment includes saturation effects and pays proper attention to the finite rise time of the laser pulse and the non-Lorentzian wings of the laser spectrum. Numerical results for the cesium atoms indicate that due to saturation effects the spin polarization is generally less than its value predicted by perturbation theory. The different saturation behavior of the ionization channels causes a saturation dip to develop in the degree of spin polarization.

I. INTRODUCTION

A number of theoretical as well as experimental studies on multiphoton processes have investigated special effects such as angular distributions of ejected photoelectrons, their spin polarization, the influence of photon correlations, etc.¹⁻¹⁴ Such experiments have become feasible in recent years owing to the availability of high power tunable lasers. Each of these experiments yields specific information about the atomic system, properties of the radiation field or both. For example, while photon correlation effects give information about the state of the exciting light,⁶ photoelectron angular distributions or spin polarization measurements—and combinations thereof—provide values for bound-free matrix elements and relative phase shifts for atomic systems.⁷ The spin polarization of an ejected photoelectron is related directly to the degree of spin-orbit coupling. The presence of such coupling causes spin mixing during the multiphoton process thus producing electrons with partial or even total polarization¹⁰ depending on the specific circumstances. Theoretical predictions for this effect have been based either on lowest-order perturbation theory¹⁰⁻¹² or on a more elaborate formalism based on the density matrix formalism¹⁵ and taking into account the hyperfine structure. The latter is particularly important when there is a resonance with an intermediate atomic state. This formalism has been successful in the interpretation of related experiments.

The motivation for the present work arises from the need to explore the modifications brought about by the intensity of the light. Although previous theories provide an adequate description of the phenomenon in the limit of weak fields, a thorough description that is applicable for a range of intensities from weak to strong is not available. Recent work on related problems in resonant multiphoton processes has shown that significant modifications can be expected as the light intensity

becomes large.^{16,17} It is also known by now that a related question often arising in connection with large intensities in resonant multiphoton processes is the effect of the laser bandwidth; and a proper description of resonance phenomena requires the appropriate treatment of this effect. If not for other reasons, only because it is not a priori evident which combination of intensity and bandwidth is most appropriate for a given specific purpose, and usually, small bandwidth implies a sacrifice of intensity.

Special attention must also be paid to the laser line shape; for Lorentzian line shapes the incoherent population of the atomic states by absorption of photons from the wings of the spectrum may dominate the ionization probability. On the other hand, such contributions become negligible for line shapes falling off faster than Lorentzian in their wings.^{18,19} Since laser line shapes do indeed fall off much faster than Lorentzian in their tails, a Lorentzian line-shape model is inadequate to describe the ionization probability and spin polarization in the presence of several interfering resonances. Closely related to the problems in context with the laser line shape are the spurious effects arising from the sudden (stepwise) turning on of the laser pulse assumed in theoretical calculations.²⁰ A laser pulse turned on instantaneously has initially a very broad bandwidth which in turn populates the atomic states irrespective of their detuning. Such a population of the states can dominate the ionization probability in a way similar to the effects arising due to the Lorentzian laser spectrum. These effects can be eliminated by taking into account the finite turning on time of the pulse.

The work presented in this paper incorporates these effects into the calculation of spin polarization in a specific resonant multiphoton process that we have chosen as an example; namely, three-photon ionization of cesium via a two-photon resonance with the $9D$ state. This is a transition

that can be reached easily with present-day tunable lasers. Since the fine-structure states $9D_{3/2}$ and $9D_{5/2}$ are separated by about 7 cm^{-1} , this problem also allows us to explore the effect of two neighboring resonant states on the saturation behavior of such processes. A process in which spin-polarized electrons are produced can always be assessed as a potential source of polarized electrons. Its merits depend on how large, predictable, and insensitive to the changes in experimental parameters the spin polarization is. Sources of spin polarized electrons, however, exist in large variety and it is not our intention to elaborate on such questions here. It is rather the fundamental aspects of the interaction that are at the focus of this work, especially since these processes can be employed in the determination²¹ of atomic parameters. In Sec. II, we present a brief description of the theory and the numerical results are presented and discussed in Sec. III.

II. THEORY

In this section we shall discuss the theory of three-photon ionization with intermediate two-photon resonances. Attention will be focused on alkali atoms where the ground state is an S state. The higher angular-momentum states ($l \neq 0$) are split due to the spin-orbit coupling. Specifically we shall consider the $9D_{3/2}$, $9D_{5/2}$ doublet as a pair of two-photon resonant intermediate states. A schematic level diagram is shown in Fig. 1 for cesium.

Because of the spherically symmetric ground state, linearly polarized light will eject unpolarized electrons after ionization. However, in the presence of circularly polarized light, the strong spin-orbit coupling will cause the electron to be

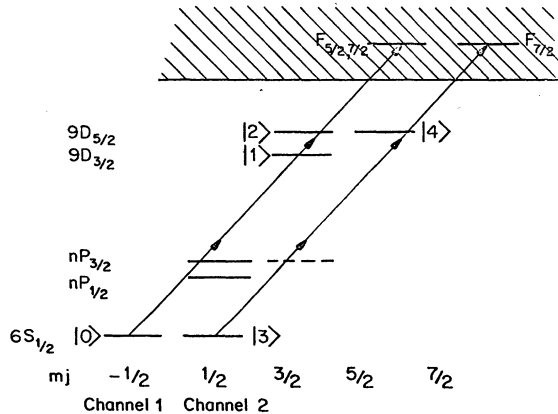


FIG. 1. Schematic level diagram for three-photon ionization in cesium via the $9D_{3/2, 5/2}$ states. Only the relevant m_j levels are shown for clarity. $nP_{1/2, 3/2}$ denote the off-resonant intermediate P states.

ejected with a definite nonzero spin polarization (SP). For this reason we shall assume light to be right circularly polarized and write the electric field vector as

$$\vec{E}(t) = E_0(t) \vec{e} e^{-i\omega t} e^{-i\phi(t)} + \text{c.c.}, \quad (1)$$

where $\vec{e}(t) = -(1/\sqrt{2})(\vec{e}_1 + i\vec{e}_2)$ represents the polarization vector, \vec{e}_1, \vec{e}_2 are unit vectors orthogonal to the direction of propagation, and ω corresponds to the center frequency of the field. $E_0(t)$ is the slowly varying amplitude of the field. To study the effects of a sudden and quasiadiabatic turning on of the pulse, we choose, following Theodosiou *et al.*,²⁰

$$E_0(t) = \begin{cases} \sqrt{t/\tau} E_0, & 0 \leq t \leq \tau \\ E_0, & t \geq \tau \end{cases} \quad (2)$$

with τ the (finite) rise time of the pulse. $\phi(t)$ is the phase of the field which is assumed to fluctuate according to the phase diffusion model (PDM).^{18,19} These fluctuations are described by the Langevin equation

$$\frac{d}{dt} \phi(t) = F(t), \quad (3a)$$

where $F(t)$ is a Gaussian stochastic force with first-order correlation function

$$\langle F(t)F(t') \rangle = b\beta e^{-\beta|t-t'|}. \quad (3b)$$

From Eq. (3b) the parameter $1/\beta$ is identified with the coherence (fluctuation) time of $d\phi/dt$, while from the correlation function

$$\langle e^{i\phi(t)} e^{-i\phi(t')} \rangle = \exp -b \left(\tau + \frac{e^{-\beta\tau} - 1}{\beta} \right), \quad (4)$$

with

$$\tau = |t - t'|,$$

the spectrum is found to be a Lorentzian with FWHM $2b$ having a cutoff at frequencies $\beta (\gg b)$. Note that in the limit $\beta \rightarrow \infty$, where $\phi(t)$ has a zero correlation time, the spectrum becomes a pure Lorentzian.

Within the dipole and rotating wave approximation the slowly varying density matrix elements²² for the system shown in Fig. 1 (averaged over the phase fluctuations) obey the following equations.

$$\frac{d}{dt} \rho_{00} = -\frac{1}{2} i (\Omega_{01} \rho_{10} - \text{c.c.}) - \frac{1}{2} i (\Omega_{02} \rho_{20} - \text{c.c.}), \quad (5a)$$

$$\frac{d}{dt} \rho_{11} = -\Gamma_1 \rho_{11} + \frac{1}{2} i (\Omega_{01} \rho_{10} - \text{c.c.}) + \frac{1}{2} i (\Omega_{12}^* \rho_{12} - \text{c.c.}), \quad (5b)$$

$$\frac{d}{dt} \rho_{22} = -\Gamma_2 \rho_{22} + \frac{1}{2} i (\Omega_{02} \rho_{20} - \text{c.c.}) - \frac{1}{2} i (\Omega_{12} \rho_{12} - \text{c.c.}), \quad (5c)$$

$$\begin{aligned} & \left(\frac{d}{dt} + i(\omega_{12} + S_{12}) + \frac{1}{2}(\Gamma_1 + \Gamma_2) \right) \rho_{12} \\ & = -\frac{1}{2} i \Omega_{10} \rho_{02} + \frac{1}{2} i \Omega_{02} \rho_{10} + \frac{1}{2} i (\Omega_{12}^* \rho_{11} - \Omega_{12} \rho_{22}), \end{aligned} \quad (5d)$$

$$\frac{d}{dt} \rho_{33} = -\frac{1}{2} i (\Omega_{34} \rho_{43} - \text{c.c.}), \quad (5e)$$

$$\frac{d}{dt} \rho_{44} = -\Gamma_4 \rho_{44} + \frac{1}{2} i (\Omega_{34} \rho_{43} - \text{c.c.}), \quad (5f)$$

$$\begin{aligned} & \left(\frac{d}{dt} - i\Delta_1 + \frac{1}{2}\Gamma_1 + 4b \frac{\beta^2}{\Delta_1^2 + \beta^2} \right) \rho_{10} \\ & = \frac{1}{2} i \Omega_{10} (\rho_{11} - \rho_{00}) - \frac{1}{2} i \Omega_{12} \rho_{20} + \frac{1}{2} i \Omega_{20} \rho_{12}, \end{aligned} \quad (5g)$$

$$\begin{aligned} & \left(\frac{d}{dt} - i\Delta_2 + \frac{1}{2}\Gamma_2 + 4b \frac{\beta^2}{\Delta_2^2 + \beta^2} \right) \rho_{20} \\ & = \frac{1}{2} i \Omega_{20} (\rho_{22} - \rho_{00}) - \frac{1}{2} i \Omega_{21} \rho_{10} + \frac{1}{2} i \Omega_{10} \rho_{21}, \end{aligned} \quad (5h)$$

$$\left(\frac{d}{dt} - i\Delta_4 + \frac{\Gamma_4}{2} + 4b \frac{\beta^2}{\Delta_4^2 + \beta^2} \right) \rho_{43} = \frac{1}{2} i \Omega_{43} (\rho_{44} - \rho_{33}). \quad (5i)$$

In writing these equations we have eliminated the intermediate off-resonant states as well as the continuum. Details of this procedure are described in Ref. 23. In Eq. (5), $\omega_{ij} = \omega_i - \omega_j$ are the differences between the atomic energies;

$$\frac{1}{2} \Omega_{i0} = \frac{1}{2} \Omega_{0i} = \sum_j \frac{\mu_{ij} \mu_{j0}}{\omega - \omega_{j0} + i\epsilon} E_0^2(t), \quad (6)$$

with $i = 1, 2$ and an analogous expression for Ω_{43} denote the two-photon transition Rabi frequencies. $\mu_{ij} = \langle i | \vec{r} \cdot \vec{\epsilon} | j \rangle$ are the atomic dipole matrix elements. The field-induced shift width functions for the various levels are given by

$$S_j - i\frac{1}{2}\Gamma_j = \sum_i \frac{|\mu_{ji} E_0(t)|^2}{-\omega + \omega_{ji} + i\epsilon} + \sum_k \frac{|\mu_{ki} E_0(t)|^2}{\omega_{jk} + \omega + i\epsilon}, \quad i = 0, 1, 2, 3, 4 \quad (7)$$

with $S_{ij} = S_i - S_j$, while

$$\begin{aligned} \frac{1}{2} \Omega_{21} = \frac{1}{2} \Omega_{12} = \frac{1}{2} (\Omega'_{12} - i\Omega''_{12}) &= \sum_i \frac{\mu_{1i} \mu_{i2}}{\omega_{1i} - \omega + i\epsilon} |E_0(t)|^2 \\ &+ \sum_k \frac{\mu_{1k} \mu_{k2}}{\omega_{1k} + \omega + i\epsilon} |E_0(t)|^2 \end{aligned} \quad (8)$$

represents Raman-type interferences between the two resonant states of channel 1.^{23,24} The detunings Δ_k are defined as $\Delta_j = 2\omega - \omega_{j0} - S_{j0}$, $j = 1, 2$ and $\Delta_4 = 2\omega - \omega_{43} - S_{43}$.

In writing Eq. (5) the averaging over the phase fluctuations has been performed using a procedure described in detail in Refs. 18 and 19. This introduces additional damping constants in Eqs. (5g)–(5i) for the off-diagonal matrix elements ρ_{10} , ρ_{20} , and ρ_{43} describing the destruction of the

atomic coherence due to the phase fluctuations. The factor of $4b$ in these damping constants arises from the relaxation constant of the second-order field correlation function. The detuning dependent cut-off factor stems from the non-Lorentzian nature of the laser line shape. For detunings smaller than the cutoff β of the frequency spectrum, these damping terms reduce to $4b$ in agreement with the result quoted for the PDM with Lorentzian spectrum. For detunings larger than β , the bandwidth dependent damping constants drop out of Eqs. (5g) through (5i). Thus a laser with a spectrum falling off faster than a Lorentzian appears monochromatic to the atom for large detunings. The description of the effect of phase fluctuations in terms of these detuning dependent damping constants is restricted to the parameter regime where the Rabi frequencies Ω_{ij} and the shifts S_{ij} are smaller than the cutoff parameter of the spectrum β . A more accurate treatment of phase fluctuations, valid for $\Omega_{ij} \gg \beta$ has been given in Ref. 19 in connection with the double optical resonance. Such a detailed calculation, however, does not seem necessary at this stage.

In Eq. (5) we have neglected spontaneous emission from the excited resonant states. This is possible if the ionization widths are larger than the spontaneous decay constants. Within this approximation, channels 1 and 2 become decoupled.

The ionization probabilities (IP) in channels 1 and 2 are given by

$$P_1 = 1 - \rho_{00} - \rho_{11} - \rho_{22} \quad (9a)$$

and

$$P_2 = 1 - \rho_{33} - \rho_{44}, \quad (9b)$$

while the total IP is given by

$$P = \frac{1}{2}(P_1 + P_2). \quad (9c)$$

For the calculation of SP, the IP for the ejected electron with its spin up ($m_s = \frac{1}{2}$) or down ($m_s = -\frac{1}{2}$) needs to be calculated. Let P_i^\pm denote the spin up (down) IP's from channel $i = 1, 2$. Angular-momentum selection rules then suggest that

$$P_2^+ = P_2, \quad P_2^- = 0.$$

Decomposing Γ_1 , Γ_2 , Ω_{12}'' into their spin up (Γ_1^+ , Γ_2^+ , $\Omega_{12}''^+$) and spin down (Γ_1^- , Γ_2^- , $\Omega_{12}''^-$) components, P_1^\pm with $P_1 = P_1^+ + P_1^-$ obey

$$\frac{d}{dt} P_1^\pm = \Gamma_1^\pm \rho_{11} + \Gamma_2^\pm \rho_{22} + 2\Omega_{12}''^\pm \text{Re} \rho_{12}. \quad (10)$$

The first two terms in (10) describe the ionization loss from states $|1\rangle$ and $|2\rangle$ while the third term is an interference contribution. The SP of

the electrons can then be expressed as

$$SP = \frac{P_1^+ + P_2^+ - (P_1^- + P_2^-)}{P_1^+ + P_2^+ + P_1^- + P_2^-} = \frac{x + y}{1 + y}, \quad (11)$$

where $x = (P_1^+ - P_1^-)/P_1$ and $y = P_2/P_1$. The parameter x is the SP in channel 1 while y denotes the ratio of the total ionization probabilities in channels 2 and 1. Equation (11) is in a form which is useful for discussion of the behavior of the SP.

The SP of the ejected electrons can now be found by solving the density matrix equations (5), assuming the electrons to be equally distributed in the two ground levels $|0\rangle$ and $|3\rangle$ at $t=0$ [$\rho_{00}(t=0) = 1 = \rho_{33}(t=0)$]. The time integral of the ionization rates \dot{P}_1^\pm together with $P_2^+ = P_2$ then yields the SP via formula (11).

III. NUMERICAL CALCULATIONS AND RESULTS

In this section we shall discuss the behavior of the SP and IP as a function of the intensity, bandwidth, the detuning from resonances, etc. Owing to the complexity of analytical solutions of Eq. (5) for the IP, we will restrict ourselves to numerical calculations. The three-photon ionization process under consideration is the $6S_{1/2} \rightarrow 9D_{3/2,5/2} \rightarrow$ continuum process in cesium. For right circularly polarized light, various atomic parameters, expressed in radians/sec are,

$$\begin{aligned} \Omega_{10} \approx \Omega_{01} &= 59.785 I, & \Omega_{02} \approx \Omega_{20} &= 35.055 I, \\ \Gamma_1 &= 9.690 I, & \Gamma_2 &= 7.611 I, \\ S_0 &= 201.364 I, & S_1 &= 101.572 I, \\ S_2 &= 95.607 I, & \Omega_{12} \approx \Omega_{21} &= 24.204 I - i1.384 I, \\ \Gamma_1^+ &= 1.384 I, & \Gamma_1^- &= 8.305 I, \\ \Gamma_2^+ &= 5.536 I, & \Gamma_2^- &= 2.076 I, \\ \Omega_{12}^{''+} &= -2.768 I, & \Omega_{12}^{''-} &= 4.152 I, \\ \Omega_{43} \approx \Omega_{34} &= 78.411 I, & \Gamma_4 &= 10.377 I, \\ S_3 &= 231.536 I, & S_4 &= 117.667 I, \end{aligned}$$

where I denotes the average intensity in W/cm^2 .

The calculations have been carried out in the fine-structure scheme. The largest hyperfine splitting of the $9D$ states is about 12 MHz.²⁵ For the on-resonance (either with $9D_{3/2}$ or the $9D_{5/2}$ state) excitation, the fine-structure scheme is justified as long as the ionization width is larger than 12 MHz or the laser duration is shorter than ~ 80 ns. Note that the spontaneous life times of the $9D_{5/2,3/2}$ states are 226 and 120 ns, respectively, and therefore longer than 80 ns. Since all of our calculations have been performed for laser durations of 5 ns, the fine-structure scheme is perfectly valid. Even if the laser duration were long the calculations would still be valid because,

at the intensities we have used, the ionization widths will be larger than 12 MHz.

As $P_2^- = 0$, electrons ionized in channel 2 will all be polarized in the spin up ($m_s = \frac{1}{2}$) direction. On the other hand, the SP in channel 1, denoted by x , depends on the photon frequency. For example, for photon frequencies close to the $D_{3/2}$ resonance, $x < 0$ because $\Gamma_1^+ < \Gamma_1^-$, while if $2\hbar\omega$ is tuned to the $D_{5/2}$ resonance, $x > 0$ because $\Gamma_2^+ > \Gamma_2^-$. Moreover, $x \rightarrow -1$ when photon frequency is very far off resonance from both the $D_{3/2,5/2}$ levels. In this case $y \rightarrow 1$ and $SP \approx 0$ as the atomic fine structure is not resolved. At the $D_{3/2}$ resonance, $P_2 \ll P_1$ and $y \rightarrow 0$ which implies $SP \approx x < 0$. On the other hand, at the $D_{5/2}$ resonance, $x > 0$ and hence $SP > 0$. Thus as one tunes $2\hbar\omega$ from the $D_{3/2}$ to $D_{5/2}$ resonance, the SP exhibits a dispersionlike behavior. This dispersionlike behavior is greatly affected by saturation as both x and y are sensitive to these effects. We shall now proceed to discuss the behavior of the SP under saturating conditions in some detail.

In Fig. 2 we have plotted SP as a function of the photon frequency (detuning) for a monochromatic laser field of intensity $I = 10^5 \text{ W}/\text{cm}^2$ and duration $T = 5$ ns. Solid and broken curves correspond to the rise time of the pulse (τ) being 0.106 ns and 1.06 ps, respectively. The dotted line represents the perturbative results of Teague and Lambropoulos,¹² which coincides with the solid line in the vicinity of the $D_{3/2}$ and $D_{5/2}$ resonances indicating excellent agreement between the present calculations and the perturbative results. Small deviations between the two results seen at larger detunings can be attributed to the fact that the effect of the background D states on the SP

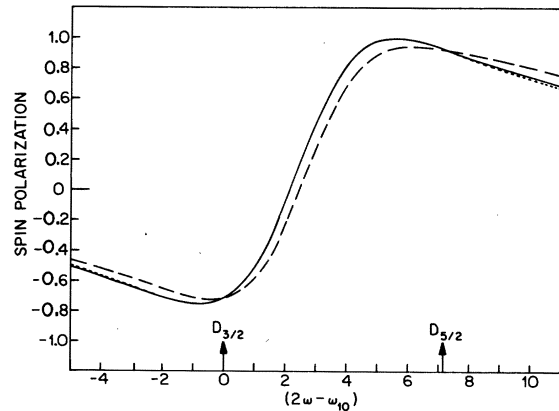


FIG. 2. Plot of SP for three-photon ionization in cesium. Solid and dashed lines are results of present calculation for $\tau = 0.106$ ns and $\tau = 1.06$ ps, respectively. Other parameters were $I = 10^5 \text{ W}/\text{cm}^2$, $b = 0$, and $T = 5$ ns. Dotted curve is the data taken from Ref. 12.

has been neglected in the present calculations while it was retained in the calculation of Ref. 12. Notice that at the position of the interference minimum between the $D_{3/2}$ and the $D_{5/2}$ state SP reaches the value unity. This is due to the fact that $P_1 \ll P_2$ in this region which implies $y = P_2/P_1 \gg 1$ and therefore $SP = 1$.

The SP is seen to be quite sensitive to the turn-on time of the pulse. For a pulse turned on sharply the off resonant SP is found to be smaller (in magnitude) than its value for an adiabatically turned on pulse. Theodosiou *et al.*²⁰ have pointed out similar behavior for the probability of multiphoton ionization. The reduction of the magnitude of the SP can be explained as follows. A sudden switching on of the pulse gives rise to a large Fourier bandwidth to the field which causes incoherent excitation of the D states of the atom. It is the contribution to the SP from the subsequent ionization of these incoherent excitations that causes a reduction of the SP. Near the $D_{3/2}$ resonance, it is the incoherent pumping of the $D_{5/2}$ state that causes the reduction of SP while similar contributions due to the $D_{3/2}$ state reduce the magnitude of the SP near the $D_{5/2}$ state. Such effects are not observable at exact resonances as the resonant contributions are orders of magnitude larger than the off-resonant, incoherent contributions. This is evident in Figs. 3(a) and 3(b) where we have plotted, respectively, the IP and SP as a function of photon frequency. In both figures, the solid and the dashed curves correspond to turning-on time of the pulse $\tau = 0.106$ ns and $\tau = 1.06$ ps, respectively. Other parameters used in these calculations were $I = 10^7$ W/cm² and $T = 5$ ns and the field is assumed monochromatic ($b = 0$). Increasing τ from 1.06 ps ($\Delta\tau \ll 1$) to about 0.1 ns ($\Delta\tau \gg 1$) decreases the IP at the minimum. This is explained by the reduction of the transient effects arising because of the sudden switching on of the pulse. The effect of these transients on the SP is exhibited in Fig. 3(b).

Thus far we have considered fields of moderate intensities ($I \leq 10^7$ W/cm²). The ionization probability has not yet saturated and the SP therefore behaves as predicted by perturbation theory. With increasing intensities, however, saturation begins to set in as P_1 and P_2 tend to unity. Significant deviations from perturbative results occur and the SP exhibits a variety of new features arising solely from the saturation as we shall see next.

Figure 4 describes the SP as a function of the detuning for various values of the intensity. Once again the field is assumed to be monochromatic ($b = 0$) and T and τ are fixed at 5 and 0.106 ns, respectively. Curves (a), (b), and (c) correspond to $I = 10^7$, 10^8 , and 10^9 W/cm². Before discussing

various effects in this figure let us note that SP is insensitive to saturation effects if only one intermediate state exists as can be seen from Eq. (10). Thus all the saturation and bandwidth effects discussed in this paper arise from the presence of other intermediate states contributing to the ionization process. Recall from Eq. (11) that x denotes the SP from channel 1 while y denotes the

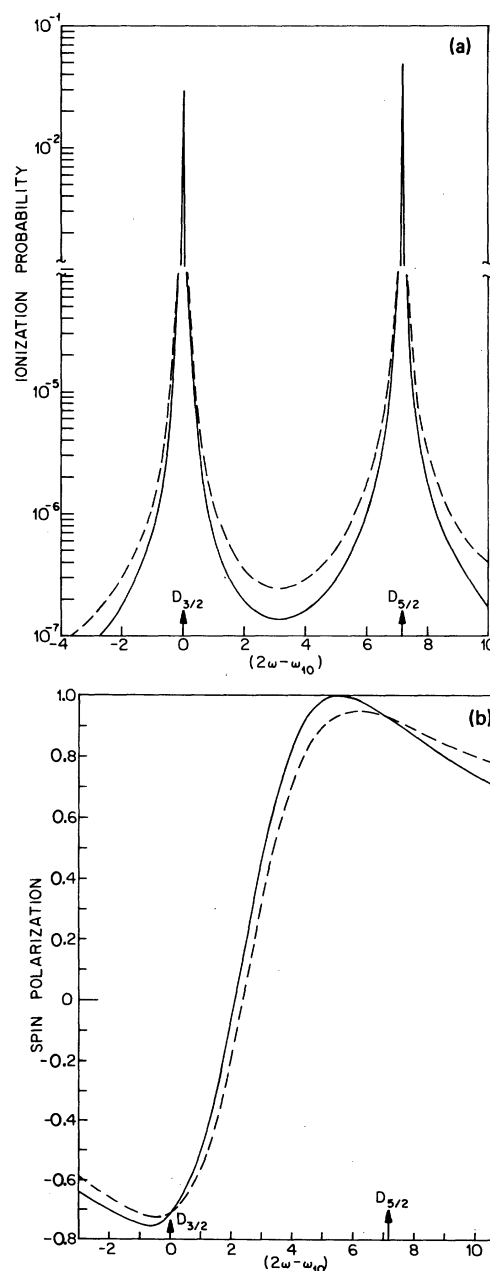


FIG. 3. Plot of the ionization probability (a) and the corresponding spin polarization (b). In both figures —: $\tau = 1.06 \times 10^{-10}$ s, and - - - -: $\tau = 1.06 \times 10^{-12}$ s. Other parameters were $I = 10^7$ W/cm², $T = 5$ ns, and $b = 0$ (monochromatic).

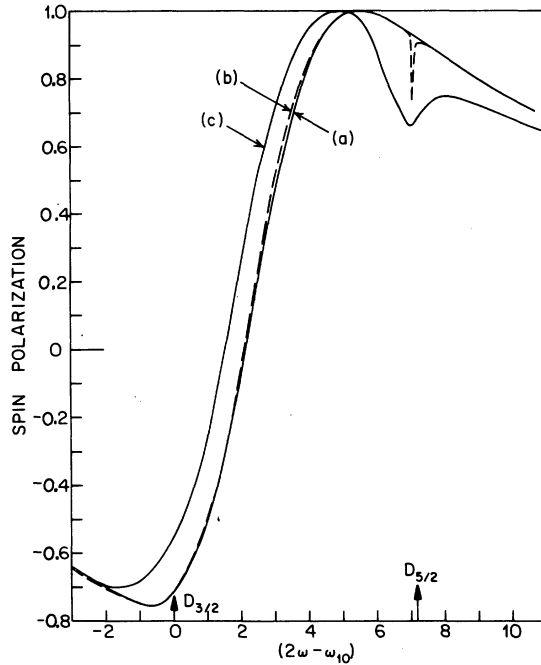


FIG. 4. SP as a function of photon frequency for monochromatic excitation ($b=0$). Curves (a), (b), and (c) correspond to $I=10^7$, 10^8 , and 10^9 W/cm², respectively. Other parameters used in these calculations were $\tau=0.106$ ns, $T=5$ ns.

ratio of IP's in the two channels which is a measure of relative saturation between the two channels. Saturation effects in channel 1 manifest themselves through the variation of x .

Let us for the moment focus our attention on the SP near the $D_{3/2}$ resonance. For $I=10^7$ and 10^8 W/cm², $P_2 \ll P_1$, which implies $y \ll 1$ and hence $SP \approx x \approx -0.7$ independent of the intensity. At 10^9 W/cm², P_1 and P_2 begin to saturate and we find that $y = 5.3 \times 10^{-2}$ while $x \approx -0.64$. Thus the SP is raised at the $D_{3/2}$ resonance. Further increases in intensity cause y to tend to unity while x increases as well and the $SP \approx (1+x)/2$ becomes positive. The increase in x at the $D_{3/2}$ resonance can be attributed to the increasing ionization via the $D_{5/2}$ state. Thus we see that the presence of a nearby off-resonant state greatly affects the SP under strong saturation conditions.

Even more spectacular behavior in the SP is seen at the $D_{5/2}$ resonance. For $I=10^7$ W/cm², SP agrees well with the perturbative results of Teague and Lambropoulos.¹² With increasing intensity, SP develops a dip at the $D_{5/2}$ resonance which deepens and widens with further intensity increases. This behavior can be explained as follows. First of all note that channel 1 has two interfering intermediate states while no such inter-

ference exists in channel 2. Thus $P_2 \gg P_1$ near the interference minimum. This corresponds to $y \gg 1$ and hence $SP=1$ at this frequency. As the intensity is increased, both P_1 and P_2 increase. Whether y will increase or decrease depends on the relative saturation of the IP in the two channels. For low intensities (less than 10^7 W/cm²) P_1 and P_2 are not saturated and hence increase at the same rate thereby keeping their ratio fixed. Thus SP also remains unchanged. At higher powers P_2 saturates faster than P_1 and thus increases at a slower rate compared to P_1 . This reduces y and the SP reflects this reduction through the minimum. At $I=10^9$ W/cm², the SP in channel 1 decreases due to increasing ionization via the $D_{3/2}$ state as the IP through the resonant $D_{5/2}$ state saturates. This causes a further deepening of the saturation dip as seen in curve (c). Under total ionization conditions, $y=1$ and hence $SP = (1+x)/2$ is positive everywhere. We have obtained such behavior at 10^{10} W/cm².

Next we examine the effect of finite bandwidth fields ($b \neq 0$) on the SP. In Fig. 5 we have plotted SP as a function of the photon frequency for various values of the bandwidth. The line shape is assumed Lorentzian ($\beta \rightarrow \infty$) and the intensity, pulse duration and its rise time are fixed at 10^8 W/cm², 5 and 0.106 ns, respectively. Curves (a)-(d) correspond to $b=0$, 0.001, 0.01, and 0.1 cm⁻¹. With increasing values of the bandwidth, the SP near the $D_{3/2}$ resonance increases (becomes less negative). Incoherent contributions to P_1 and P_2 due to resonant absorption of photons from the wings of the laser explain this effect. Such contributions are more significant in P_2 than in P_1 because in P_1 , the resonant ionization via the $D_{3/2}$ state masks any changes in the effect of the $D_{5/2}$ level while no such overshadowing exists in P_2 . Hence y increases with increasing bandwidth thereby increasing the SP. Exactly an opposite effect occurs near the $D_{5/2}$ resonance where the incoherent contributions due to the off-resonant $D_{3/2}$ state increase P_1 and hence reduce y . Thus SP decreases in the region between the $D_{3/2}$ and $D_{5/2}$ level.

The on resonance SP at the $D_{5/2}$ level exhibits interesting behavior as a function of the bandwidth. With increasing values of b , the SP first decreases, then it begins increasing again and finally becomes flat with further increases in the bandwidth. The optimum value of b lies in the region where b is of the order of magnitude of the Rabi frequency. A further increase of b beyond this value causes a destruction of the coherence in the bound-bound transition. This reduces the IP, the saturation and hence SP increases reflecting an increase in y . For $b \gg \Omega$ ionization proceeds

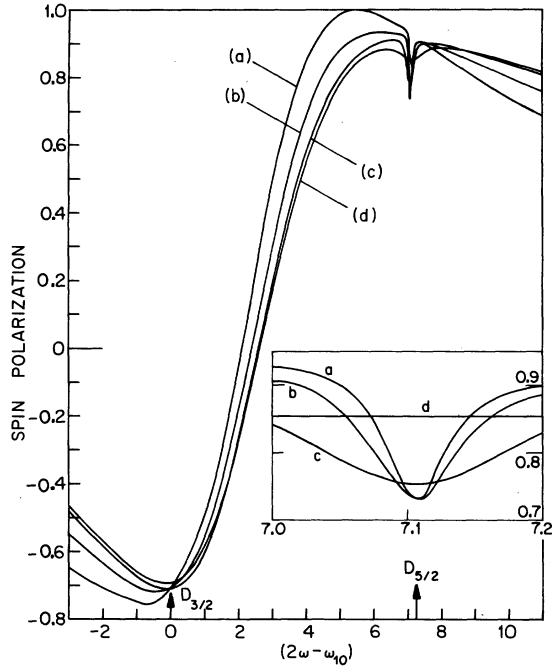


FIG. 5. SP for excitation by nonmonochromatic fields ($b \neq 0$). Laser line shape is assumed to be Lorentzian. Curves (a)–(d) correspond to $b = 0, 0.001, 0.01, 0.1 \text{ cm}^{-1}$, respectively, while $I = 10^8 \text{ W/cm}^2$, $T = 5 \text{ ns}$, and $\tau = 0.106 \text{ ns}$ for all the curves. The inset shows in detail the SP at the $D_{5/2}$ resonance.

via simple rate equations which yields a flat resonance shape for the SP. We have seen such behavior for bandwidths beyond a few wave numbers.

The above calculations have been performed assuming a Lorentzian laser line shape. Realistically, the line shape may be Lorentzian up to a few laser bandwidths around the center but falls off much faster in their wings. Therefore incoherent contributions from the far wings of a Lorentzian will be unphysically high. In a more realistic calculation, however, such contributions are negligible. We demonstrate this using the non-Lorentzian line-shape model described in Sec. II to calculate the SP. The results are shown in Fig. 6 where the SP is plotted as a function of the photon frequency for $\beta = 0.1, 1, 10$, and 1000 cm^{-1} . Recall that the parameter β characterizes the shape of the laser spectrum; namely, for finite values of β , the line shape is Lorentzian with FWHM $2b$ having a cutoff at $\beta (\gg b)$ while in the limit $\beta \rightarrow \infty$ the spectrum becomes pure Lorentzian. Decreasing β reduces the incoherent contributions discussed in connection with Fig. 5 and therefore decreases the off-resonance SP near

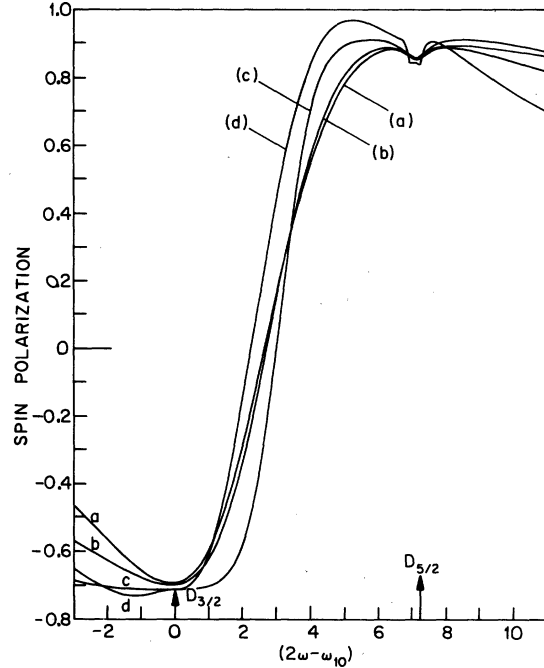


FIG. 6. Effect of the non-Lorentzian line shape on the spin polarization. These curves are plotted for $b = 0.1 \text{ cm}^{-1}$, $T = 5 \text{ ns}$, $\tau = 1.06 \times 10^{-10} \text{ s}$, and $I = 10^8 \text{ W/cm}^2$. Curves (a) through (d) correspond to $\beta = 1000, 10, 1$, and 0.1 cm^{-1} , respectively.

the $D_{3/2}$ resonance, while increasing the SP near the $D_{5/2}$ resonance. Exactly on resonance, the ionization process is insensitive to the line shape as the line shape looks Lorentzian of FWHM $2b$ at the center. Hence SP remains constant at $D_{3/2}$ and $D_{5/2}$ resonances. For smaller β , off-resonance SP tends towards the monochromatic value while for $\beta \rightarrow \infty$ the behavior obtained for a Lorentzian line-shape field is recovered.

IV. CONCLUSIONS

We have discussed the behavior of the photoelectron spin polarization in a particular three-photon ionization process. As far as the specific process and atom are concerned, the calculation is realistic and aside from minor detailed adjustments it could be compared with experimental results if they became available. Many of the results, however, are of much more general significance and are expected to be qualitatively valid in other processes as well. The SP has been found to be lower than predicted by perturbation-

theory results reported earlier. Moreover, the SP at the intermediate $D_{5/2}$ resonance has been shown to develop a dip due to the difference in the degree of saturation of the IP in the two channels. Thus saturation is seen to have a significant influence on the SP. But in resonant processes one must also be concerned with the effect of the laser bandwidth and line shape. Our analysis has shown the importance of that effect. As in previous work concerned with the effect of line shape under saturation conditions, we have found that a Lorentzian line shape can introduce unphysical effects due to its high wings. Through explicit calculations with non-Lorentzian line shapes, we have shown how such unphysical effects are eliminated.

The type of calculations and effects presented in this paper are relevant not only to questions of SP but also to other resonant multiphoton processes such as those involved in recent experiments²¹ aimed at the determination of atomic parameters. It is our feeling that further calculations along similar lines will be necessary as the interplay between theory and experiment leads to questions of finer detail in such measurements.

ACKNOWLEDGMENT

The authors acknowledge the financial support of the Österreichische Fonds zur Förderung der Wissenschaftlichen Forschung under Contract No. 3291.

*On leave of absence from the University of Southern California, University Park, Los Angeles, California 90007.

¹P. Lambropoulos, in *Advances in Atomic and Molecular Physics* (Academic, New York, 1976), Vol. 12, p. 87.

²C. Lecompte, G. Mainfray, C. Manus, and F. Sanchez, *Phys. Rev. Lett.* **32**, 265 (1974); *Phys. Rev. A* **11**, 1009 (1975).

³J. C. Hansen, T. A. Duncanson, Jr., Ring-Ling Chien, and R. S. Berry, *Phys. Rev. A* **21**, 272 (1980).

⁴M. Lambropoulos and P. Lambropoulos, in *Electron and Photon Interactions with Atoms*, edited by H. Kleinpoppen and M. R. C. McDowell (Plenum, New York, 1976).

⁵M. R. Cervenak and N. R. Isenor, *Opt. Commun.* **10**, 280 (1974).

⁶G. S. Agarwal, *Phys. Rev. A* **1**, 1445 (1970).

⁷M. Lambropoulos and R. S. Berry, *Phys. Rev. A* **8**, 855 (1973).

⁸V. L. Jacobs, *J. Phys. B* **5**, 2257 (1972); **6**, 1461 (1973).

⁹Y. Gontier and M. Trahin, *J. Phys. B* **8**, L179 (1975); **12**, 2123 (1979).

¹⁰P. Lambropoulos, *Phys. Rev. Lett.* **28**, 585 (1972); **30**, 413 (1973); and *J. Phys. B* **6**, L319 (1973).

¹¹P. Lambropoulos and M. R. Teague, *J. Phys. B* **9**, 587 (1976).

¹²M. R. Teague and P. Lambropoulos, *J. Phys. B* **9**, 1251 (1976).

¹³N. B. Delone and M. V. Fedorov, *Sov. Phys.—Usp.* **22**, 252 (1979) and references therein.

¹⁴R. Parzynski, *J. Phys. B* **13**, 469 (1980).

¹⁵G. Nienhuis, E. H. A. Granneman, and M. J. Van der Wiel, *J. Phys. B* **11**, 1203 (1978).

¹⁶B. L. Beers and L. Armstrong, Jr., *Phys. Rev. A* **12**, 2447 (1975).

¹⁷A. T. Georges and P. Lambropoulos, *Phys. Rev. A* **18**, 587 (1978).

¹⁸P. Zoller and P. Lambropoulos, *J. Phys. B* **12**, L547 (1979).

¹⁹S. N. Dixit, P. Zoller, and P. Lambropoulos, *Phys. Rev. A* **21**, 1289 (1980).

²⁰C. E. Theodosiou, L. Armstrong, M. Crance, and S. Feneuille, *Phys. Rev. A* **19**, 766 (1979).

²¹K. Kollath, *J. Phys. B* **13**, 2901 (1980).

²²A. T. Georges, P. Lambropoulos, and J. H. Marburger, *Phys. Rev. A* **15**, 300 (1977).

²³S. N. Dixit and P. Lambropoulos, *Phys. Rev. A* **21**, 168 (1980).

²⁴P. Knight, *Opt. Commun.* **31**, 148 (1979).

²⁵G. Belin, L. Holmgren, and S. Swanberg, *Phys. Scr.* **14**, 39 (1976).